

Information Processing by Neuron Populations in
the Central Nervous System:
Mathematical Structure of Data and Operations

Martin N. P. Nilsson
RISE Research Institutes of Sweden,
P.O.B. 1263, SE-164 29 Kista, Sweden
cns-information-processing@drnil.com
ORCID: 0000-0002-7504-0328



January 2, 2024

Abstract

In the intricate architecture of the mammalian central nervous system, neurons form populations. Axonal bundles communicate between these clusters using spike trains. However, these neuron populations' precise encoding and operations have yet to be discovered.

In our analysis, the starting point is a state-of-the-art mechanistic model of a generic neuron endowed with plasticity. From this simple framework emerges a subtle mathematical construct: The representation and manipulation of information can be precisely characterized by an algebra of convex cones.

Furthermore, these neuron populations are not merely passive transmitters. They act as operators within this algebraic structure, mirroring the functionality of a low-level programming language. When these populations interconnect, they embody succinct yet potent algebraic expressions. These networks allow them to implement many operations, such as specialization, generalization, novelty detection, dimensionality reduction, inverse modeling, prediction, and associative memory.

In broader terms, this work illuminates the potential of matrix embeddings in advancing our understanding in fields like cognitive science and AI. These embeddings enhance the capacity for concept processing and hierarchical description over their vector counterparts.

Significance statement: This research delves into the intriguing interplay between mathematics, neurobiology, and cognitive processes. At its core, the paper investigates how the brain might represent and organize knowledge using mathematical structures known as convex cones. These structures are proposed as a bridge between the raw, biological workings of the brain and our high-level cognitive perceptions. The findings highlight the potential of neuron populations in the brain to carry out complex operations, much like how a computer processes information. Moreover, the study touches on the possible existence of a “brain language” spoken by neuron circuits, offering insights into both artificial intelligence and our understanding of the human mind.

Keywords: Population code, mechanistic model, invariant, algebra of convex cones, matrix embedding, non-negative weights, sparsity, adaptive filter, correlation, plasticity.

MeSH 2023 terms: Neurons [A08.675], Neurological Models [E05.599.395.642], Concept Formation [F02.463.785.233], Learning [F02.463.425], Computational Biology [H01.158.273.180], Cognitive Neuroscience [F04.096.628.255.500, H01.158.610.030], Artificial Intelligence [G17.035.250,L01.224.050.375].

PhySH 2023 terms: Biological information processing, Neural basis of learning & memory, Neural encoding, Neuroplasticity, Biological neural networks.

1 Introduction

1.1 The quest for the elusive invariant

Neurons in the mammalian central nervous system (CNS) group into populations of neurons with similar functions. These ensembles communicate via bundles of axons, conveying information by spike trains. Whereas the pioneering scientist John von Neumann primarily believed the information was encoded into single spike trains, at the very end of his final work *The Computer and the Brain* [72, p. 81], he recognized the possibility of encodings based on correlations *between* spike trains: “*It is [...] perfectly plausible that certain (statistical) relationships between [...] trains of pulses should also transmit information. In this connection it is natural to think of various correlation-coefficients, and the like.*” It has indeed become increasingly clear that to resolve neuronal communication, it is necessary to understand how entire populations encode information [3, 59, 60], and accumulating evidence suggests this encoding is related to correlations between neurons [54, 33].

The integrity of information traversing a population must be preserved, as any aberration would compromise its processing. The challenge of maintaining stable invariants in an unreliable and noisy system like the CNS has been a longstanding question, also pondered by von Neumann [71]. Perkel and Bullock [56] coined the term *transformation invariance*. Pellionisz and Llinás [55] proposed and explored mathematical tensors—invariants under coordinate transformation—constituting one possible formulation of the information transmission through a population. Other prominent researchers emphasizing the significance of invariance are MacLennan [42] and Kumar et al. [36].

This paper focuses on correlation-related invariants. Initially, we examine a basic neuron model to gain insights into the behavior of populations and potential invariants. Subsequently, we apply a similar approach using a state-of-the-art, biologically accurate mechanistic neuron model with plasticity, which is conservative in the sense that it is non-speculative and strictly grounded in well-established neurobiological knowledge. This leads to a mathematical structure with a surprisingly powerful computational interpretation.

1.2 A simple population model

We temporarily adopt the classical simplistic model of a neuron that produces a weighted sum of its inputs. This article presents all communication between neurons, including the inputs $x_k(t)$ and output $z(t)$, as *spike rates*. Using standard signal processing terminology, $x_k(t)$ and $z(t)$ are *signals*, that is, time-variable functions.

For this introduction, we assume that signals are *pseudo-static*, meaning they change so slowly that we can consider them piece-wise constant. We will often omit the time parameter t in the following unless there is a need to specify it explicitly. We can write

$$z = \sum_{k=1}^n w_k x_k, \quad (1)$$

where w_k are the synaptic weights. Although this traditional model greatly oversimplifies the neuron’s capabilities, it suffices for introducing our approach. A population of m neurons (Fig. 1) can be described as a matrix-vector multiplication,

$$\mathbf{z} = W^T \mathbf{x}, \quad (2)$$

where $\mathbf{x} = (x_1, x_2, \dots, x_n)^T$ is the vector of inputs, $\mathbf{z} = (z_1, z_2, \dots, z_m)^T$ is the vector of outputs, and W is the $n \times m$ matrix of synaptic weights.



Figure 1: **Interconnected neuron populations.** We often envision neuron populations as orderly connected, as depicted in the image on the left. While this may characterize the peripheral nervous system (PNS), the image on the right portrays the central nervous system (CNS) more adequately. The absence of correlation between neighboring neurons evidences the irregularity of connections in the CNS.

1.3 Messages

We use the term *message* to describe an instantaneous vector $\mathbf{x}(t)$ representing both sensory data arriving from the peripheral nervous system (PNS) and internal information from the central nervous system (CNS). We are interested in finding invariants of the matrix multiplication (2) that preserve properties of \mathbf{x} in \mathbf{z} .

In the PNS, the mean value of \mathbf{x} could be a straightforward invariant given a somatotopic organization and strong correlation among adjacent neurons. As a result, populations of neurons having similar input signals will also have similar output signals.

However, in the CNS, adjacent neurons are essentially uncorrelated, as evidenced by various studies [13, 14, 45, 81]. Finding an invariant becomes challenging, especially given the seemingly stochastic connectivity between populations in the CNS (Fig. 1, right), which allows an input message \mathbf{x} to be mapped by W to potentially any output message \mathbf{z} .

1.4 The invariant

Rather than singular messages, invariants require sequences of messages represented geometrically as sets of points. While it might be tempting to label such an information-carrying invariant as a “concept”, we simply refer to it as an “invariant”, leaving more

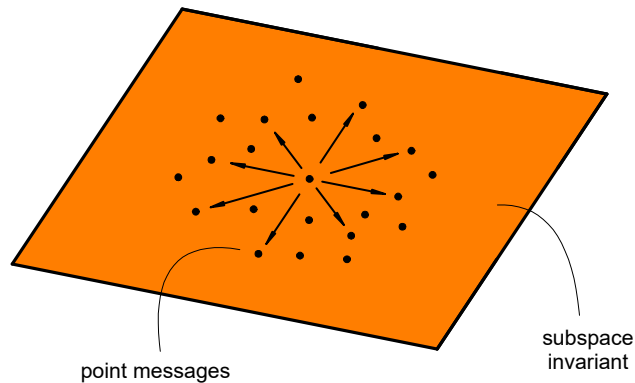


Figure 2: **Messages and invariants.** Geometrically, instantaneous spike rates are points in a subspace, where the points represent messages, and the subspace represents an invariant. Messages are not invariants.

speculative interpretations for the discussion in Sect. 7.1. One straightforward candidate for the invariant is the *subspace* spanned by these points (Fig. 2). This subspace maintains its nature even after matrix multiplication and retains its relations with other subspaces. Messages form a “cloud” with the invariant as its spanned subspace, where the eigenvectors of the message covariance matrix establish a basis for the subspace. In addition, this invariant is biologically plausible and achievable by biological neurons.

The historical difficulty of finding a transformation invariant may partly be due to the possibility of two different population coding systems for the PNS and the CNS. While the PNS has a well-known topographic organization of neuronal connections, the CNS loses this topographic mapping, and connections between populations diffuse [7, 37, 62, 73].

1.5 Sparsity

The importance of sparsity, characterized by many components in the message vector being zero, has been discussed by several authors [18, 51, 15]. It is a feature observed experimentally in the nervous system [19, 52, 40, 58, 79] and is essential for multiple reasons.

Firstly, while at most n messages in \mathbb{R}^n are linearly independent, the number of messages encodable into \mathbb{R}^n is exponential in n if the messages are sparse, and if we allow a small, non-zero probability of messages not being perfectly orthogonal, according to the Johnson-Lindenstrauss lemma [27, 8]. As a result, n dimensions can incorporate a vast number of invariants formed from sequences of messages with a negligible risk of confusion.

Another, more subtle reason is that sparsity maintains the orthogonality between messages with a high probability after crossing a neuron population. This property is vital for an algebra of invariants, and we delve into it more thoroughly in Sect. 2.5 dealing with the activation function.

Additional benefits of sparsity include simplified noise reduction and, for biological neurons, reduced metabolic activity and energy consumption.

1.6 An algebra of invariants

The set of linear subspaces of the Euclidean space \mathbb{R}^n forms an *algebra of subspaces* equipped with several operations, including *intersection*, *sum*, *projection*, and *rejection*. As we shall see in Sect. 3, neuron populations can perform generalizations of these operations, thereby implementing an algebra of invariants having a powerful *computational interpretation*. The algebra describes the mathematical structure underlying computation by neuron populations serving a role similar to hardware function blocks of a computer.

1.7 Outline of the paper

Overall, in this paper, we explore how neuron populations implement an algebra of invariants for *communication*, *processing*, and *storage* of information.

An aim is to present the approach in an accessible way by initially considering the case of a classical simple neuron model with pseudo-static inputs, requiring only linear algebra and allowing easy geometric visualization. In Sect. 2, we look at the algebra of subspaces and its basic operations. This algebra is scrutinized because it is helpful in its own right and hints at what to expect from a generalization to convex cones.

Introducing a full-fledged mechanistic model of neurons and populations in Sect. 3 necessitates additional mathematical tools for handling time-variable signals. Sect. 4 generalizes the algebra of subspaces to convex cones, capitalizing on the non-negativity of synaptic weights. The following section, Sect. 5, concretely illustrates the capability of neuron populations to implement basic algebraic operations, composite operations, conditionals, and memory operations.

Finally, we summarize the main results (Sect. 6), discuss related research and associated issues in cognitive science and artificial intelligence (Sect. 7), and conclude the paper (Sect. 8). Most mathematical derivations are confined to sections marked with asterisks for enhanced readability. A cursory reading can bypass these sections without compromising the comprehension of the paper.

2 Representation and manipulation of subspaces

This section provides a detailed explanation of the representations of and operations on subspaces, including how these can be implemented by matrices and matrix operations, facilitating computer implementation, experimentation, and visualization of algebras of subspaces.

In the following, lowercase letters denote subspaces and uppercase matrices while boldface denote vectors. The notation $A \sim B$ says that A and B represent the same subspace. If a is a subspace and A a matrix representing it, $a \sim A$ is equivalent to $a = \text{Col}(A) = \{\mathbf{x} \in \mathbb{R}^n | \mathbf{x} = A\boldsymbol{\theta}, \boldsymbol{\theta} \in \mathbb{R}^m\}$, also known as the *column space* or *range* of the matrix A . The *linear hull* \bar{s} of a set of vectors s is the set of linear combinations of vectors in s .

2.1 Representations of subspaces

One way to represent a subspace $s \subseteq \mathbb{R}^n$ is by an $n \times m$ matrix

$$A = (\mathbf{a}_1 \quad \mathbf{a}_2 \quad \dots \quad \mathbf{a}_m) \in \mathbb{R}^{n \times m} \quad (3)$$

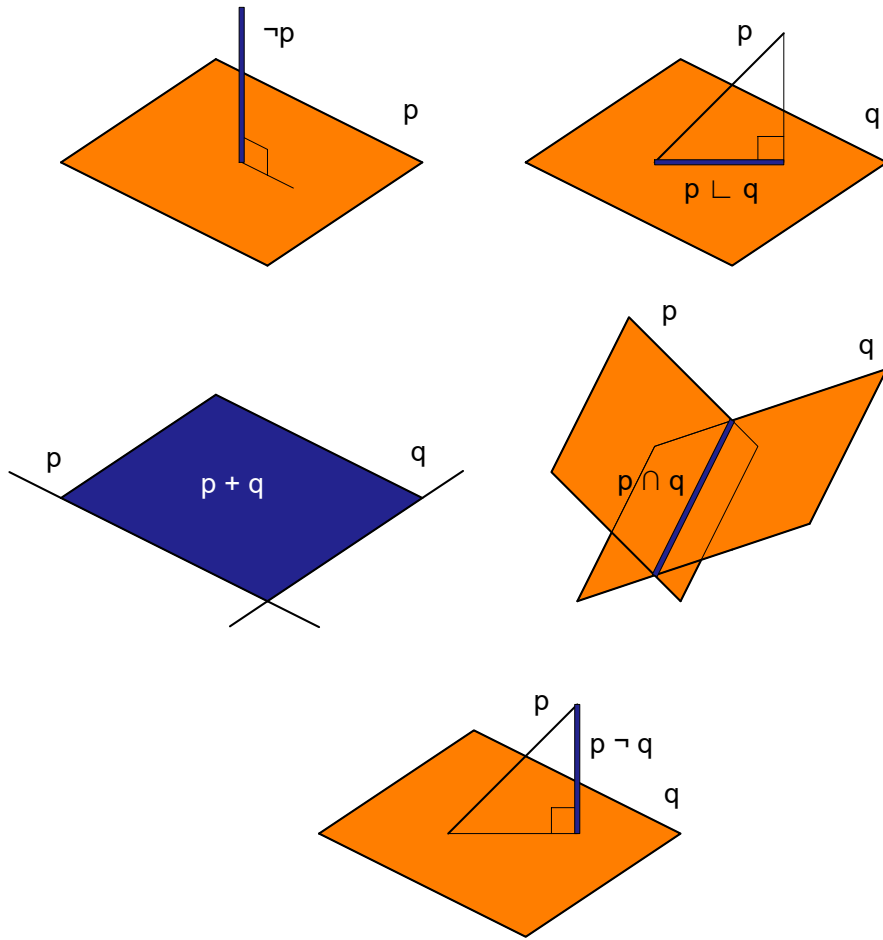


Figure 3: **Basic operations on subspaces.** The five basic operations on subspaces are illustrated in left-to-right and top-down order: *orthogonal complement*, *orthogonal projection*, *sum*, *intersection*, and *orthogonal rejection*.

of column vectors $\{\mathbf{a}_1, \mathbf{a}_2, \dots, \mathbf{a}_m\} \subseteq \mathbb{R}^n$ whose linear hull spans the subspace s ,

$$s = \overline{\{\mathbf{a}_1, \mathbf{a}_2, \dots, \mathbf{a}_m\}} = \text{Col}(A).$$

This representation of s is not unique, but if we restrict the matrices to *orthogonal projection matrices* P , which satisfy $P^2 = P = P^T$, we obtain a canonical representation. The matrix P can always be generated from A by $P = AA^+$, where A^+ denotes the Moore-Penrose pseudoinverse of A . Sect. 2.2 shows that $A \sim AA^T \sim AA^+$.

We can interpret the matrix A statistically as a collection of data vectors: Suppose that the m observation vectors \mathbf{a}_k in (3) are independent and identically distributed samples of an n -dimensional stochastic variable \mathbf{a} with a zero-mean probability distribution. Then AA^T is approximately proportional to the *covariance matrix*, $AA^T \approx m \text{Cov}(\mathbf{a})$. We can think of the subspace as a “playground” for messages. The eigenvectors of the covariance matrix having the largest eigenvalues correspond to the most fluctuating directions inside the subspace.

2.2 * Derivation of subspace representation

It is well known that any matrix A can be decomposed by singular-value decomposition (SVD) as the matrix product $U\Sigma V^T$, where U and V are orthonormal matrices, and Σ is a diagonal matrix.

$$\begin{aligned}
\text{Col}(A) &= \{\mathbf{x} = A\boldsymbol{\theta} \mid \boldsymbol{\theta} \in \mathbb{R}^m\} \\
&= \{\mathbf{x} = U\Sigma V^T\boldsymbol{\theta} \mid \boldsymbol{\theta} \in \mathbb{R}^m\} \\
&= \{\mathbf{x} = U\Sigma\boldsymbol{\theta} \mid \boldsymbol{\theta} \in \mathbb{R}^m\} \\
&= \{\mathbf{x} = U\Sigma\Sigma^T\boldsymbol{\theta} \mid \boldsymbol{\theta} \in \mathbb{R}^n\} \\
&= \{\mathbf{x} = U\Sigma\Sigma^T U^T\boldsymbol{\theta} \mid \boldsymbol{\theta} \in \mathbb{R}^n\} \\
&= \text{Col}(AA^T),
\end{aligned}$$

implying that $A \sim AA^T$. Replacing Σ^T with Σ^+ above similarly leads to $\text{Col}(A) = \text{Col}(AA^+)$ and $A \sim AA^+$.

2.3 Basic operations on subspaces

Five basic operations can be performed on subspaces, as shown in Fig. 3. Each of these operations has an intuitive geometric interpretation. We defer speculative conceptual interpretations of the operations to the discussion in Sect. 7.1. Below, we describe the operations in detail, introduce symbols for them, and define them in terms of matrix operations. Given that P and Q are matrices corresponding to p and q , respectively, the five basic operations are *orthogonal complement* (unary symbol ' \neg '), *orthogonal projection* (binary ' \perp '), *intersection* (binary ' \cap '), *sum* (binary ' $+$ '), and *orthogonal rejection* (binary ' \dashv '). The operator symbols precedence order is assumed to be, from high to low, ' \neg ', ' \perp ', ' \cap ', ' $+$ ', ' $=$ ', ' \subseteq ', and ' \sim '. All complements, projections, and rejections in this paper are assumed orthogonal, so this will rarely be explicitly stated.

The basic operations are defined as

- **Complement:** The *complement* of subspace p is the set of all vectors perpendicular to p . It can be computed by the matrix subtraction

$$\neg p \sim I - PP^+,$$

where I is the $n \times n$ identity matrix.

- **Sum:** The *sum* operation computes all possible sums of a vector from p and one from q . *Sum* can be computed by matrix addition,

$$p + q = \text{Col}([P \ Q]) \sim [P \ Q] \begin{bmatrix} P^T \\ Q^T \end{bmatrix} = PP^T + QQ^T,$$

where $[P \ Q]$ is the matrix created by juxtaposing P and Q horizontally. *Sum* does not distribute over *intersection*, so in general,

$$(p + q) \cap r \neq (p \cap r) + (q \cap r).$$

Sum and *complement* are the only basic operations that can potentially increase the subspace dimensionality beyond the maximum dimensionality of their inputs.

- **Projection:** The *projection* operation can be expressed as

$$p \perp q \sim QQ^+PP^+ \sim QQ^+P.$$

- **Rejection:** The *rejection* operation can be defined as the projection of p on the complement of q ,

$$p \neg q = p \perp (\neg q) \sim (I - QQ^+)P.$$

Projection can be defined in terms of *rejection* because

$$\begin{aligned} p \neg (p \neg q) &\sim [I - (I - QQ^+)PP^+]P \\ &= P - (I - QQ^+)P \\ &= QQ^+P \\ &\sim p \perp q. \end{aligned}$$

- **Intersection:** The *intersection* operation outputs the vectors belonging to both p and q . *Intersection* can be defined in terms of *complement* and *sum*, because the complement of the sum of p and q must be perpendicular to both p and q :

$$\neg(p + q) = (\neg p) \cap (\neg q),$$

so

$$\begin{aligned} p \cap q &= \neg(\neg p + \neg q) \\ &\sim I - (2I - PP^+ - QQ^+)(2I - PP^+ - QQ^+)^+. \end{aligned}$$

Intersection can also be expressed in terms of *sum* and *rejection* (Sect. 4.4.3):

$$p \cap q = (p + q) \neg (q \neg p + p \neg q).$$

2.4 Relations between subspaces

We say that a subspace a is *empty* if it contains only the origin, $a = \{\mathbf{0}\}$.

A *partial order* of subspaces is crucial for forming hierarchies of invariants. It can be seen as an *is-a* relation, a conditional, or an entailment. The obvious ordering is to define $p \preceq q$ if and only if p is a subset (subspace) of q , $p \subseteq q$. We can determine this by checking if the rejection of q from p is empty, *i.e.*, p is a subspace of q if and only if $p \neg q = \{\mathbf{0}\}$.

However, such a partial ordering is unsatisfactory in the algebra of subspaces because if p is a subspace of q , *either p and q are identical, or q must be of higher dimensionality than p* . This limitation renders the partial ordering rather coarse, especially because of the sparsity requirement, and is an inevitable weakness of subspace invariants. In Sect. 4.3, we will see that the generalization of invariants from subspaces to convex cones eliminates this dilemma by allowing a more fine-grained ordering, including same-dimensional invariants.

In theory, it is easy to compare subspaces for *equality* using the projection matrix because this is a canonical representation. Hence, two subspaces are equal if their projection matrices P and Q are equal. In practice, however, subspaces are rarely precisely equal, so we need a *graded* comparison. Such a comparison of subspaces can be achieved by an inner product $\langle P, Q \rangle \triangleq \sum_{i,j} p_{ij}q_{ij} = \text{tr}(P^T Q)$ of projection matrices P

and Q , where the function $\text{tr}(\cdot)$ denotes the trace. Gleason’s theorem shows this is the only method with desirable properties [70]. The inner product defines the associated matrix norm—the Frobenius norm—by $\|A\|_F \triangleq \sqrt{\langle A, A \rangle}$, so analogous to the vector inner product, we can compare subspaces p and q represented by matrices P and Q , respectively, by

$$\cos \theta = \frac{\langle P, Q \rangle}{\|P\|_F \|Q\|_F}.$$

where a magnitude near one indicates that the subspaces are similar.

2.5 The activation function and retaining sparsity

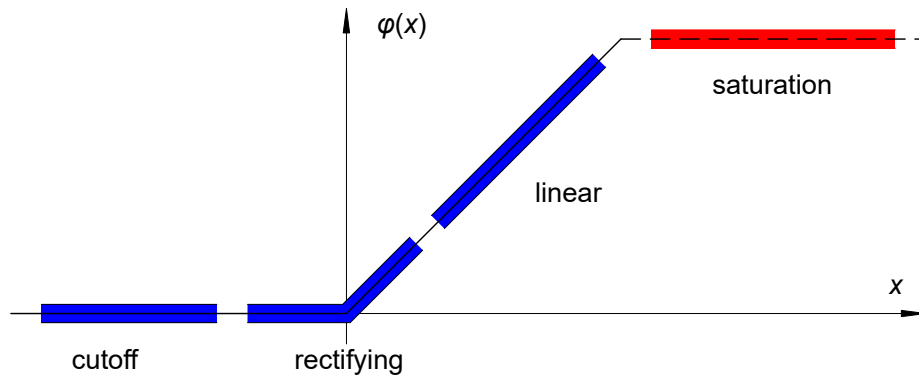


Figure 4: **The activation function.** The activation function $\varphi(\cdot)$ operates in three different ranges: *cutoff*, where it is zero; *rectifying*, where it operates as a soft-threshold function; and *linear*, where it is a purely linear function of the argument. Although there is a fourth range, *saturation*, it is irrelevant in practice due to the potential damage it causes to biological neurons through overexcitation (excitotoxicity).

In the classical neuron model (1), an *activation function* $\varphi(\cdot)$ is often applied to the output. The activation function is a soft-threshold function and has the three principal ranges of operation *linear*, *rectifying*, and *cutoff* (Fig. 4). In a biological neuron, the activation function is a biophysical consequence of the spike generation mechanism [47].

Thus far, we considered the neuron to operate predominantly within the activation function’s linear range. The rectifying range, however, has the essential function to ensure sparse representations. Populations create representations of invariants by adapting weights based on sequences of messages. These messages are typically noisy, meaning the invariant representation may become excessively high-dimensional and needs trimming. A similar situation exists after a *sum* operation. Within the rectifying range, the activation function applies a soft threshold that only permits the largest output components to pass through, thereby eliminating noise and preserving the sparsity of the population’s output.

Sparsity is crucial for maintaining the orthogonality of messages when traversing neuron populations. Consider two interconnected populations, A and B (Fig. 1, right) to see this. Intuitively, we can see the connection as a permutation with some “softening” due to the axon splitting into collaterals terminating at multiple neurons. More

formally, suppose that A sends a message \mathbf{x}_1 to B containing n neurons. Let \mathbf{x}_1 be sparse, having only $m \ll n$ non-zero components. If each axon has p collaterals uniformly randomly connecting to neurons in B, then \mathbf{x}_1 will on the average connect to approximately $q = n[1 - (1 - 1/n)^{mp}] \approx n[1 - \exp(-mp/n)]$ different neurons in B. The activation function will separate the $k \ll n$ strongest components and pass them on as outputs. Consider another sparse message \mathbf{x}_2 , uncorrelated with and orthogonal to \mathbf{x}_1 . While it may accidentally connect to approximately q^2/n overlapping neurons in B, the activation function can again reduce the output to k components *independently of \mathbf{x}_2 as long as \mathbf{x}_1 and \mathbf{x}_2 are uncorrelated*. So, given the absence of correlations, near orthogonality is retained with the same probability as two sparse (k out of n non-zero components) random messages being nearly orthogonal.

3 Mathematical abstraction of neuron populations

3.1 A generic mechanistic neuron model

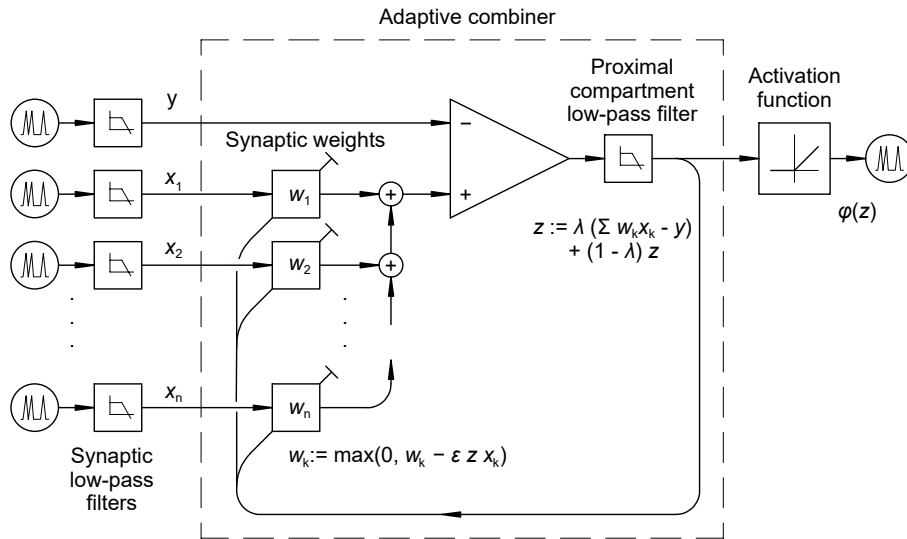


Figure 5: **A generic neuron with plasticity.** The neuron operates as an adaptive filter or combiner with internal feedback, where weights are non-negative. The mechanistic model above derives from experiments and known properties of ion channels [46]. The decay factor λ characterizes low-pass filtering of the output z . The proximal compartment comprises the soma and proximal sections of the dendrites.

This section reviews a conservative mechanistic model of a generic neuron with plasticity [46] and uses it to formulate a population model. Here, “conservative” means that the model is derived solidly from established knowledge of biological neurons and ion channel properties and contains no speculative or phenomenological additions. The generic neuron is similar to the hippocampal CA1 pyramidal cell because this cell is representative of a large class of CNS neurons and has been extensively studied. It is the foundation for building the model of neuron populations and their ability to process information.

There are at least five significant reasons for relying on a mechanistic and non-speculative neuron model:

Foundation in Established Principles: The mechanistic model is rooted in well-established scientific knowledge of biological neurons. This solid foundation increases confidence in the model’s validity and its explanations.

Predictive Power: Since the mechanistic model is grounded in established principles, it has robust predictive power. It allows predictions about yet unobserved phenomena, allowing further testing and validating the model.

Explanatory Insights: The mechanistic model provides a detailed understanding of how and why the neuron behaves the way it does. For example, breaking down the neuron into a formulation as an electrical equivalent circuit directly reveals its underlying plasticity rule.

Causal Explanation: The mechanistic model enables causal explanations. Not only does it explain the correlations observed in neuron signaling, but it also elucidates the causal mechanisms behind the observed phenomenon.

Addressing Complex Systems: The mechanistic approach is especially suitable for studying networks of many composite populations whose relations are intricate. The mechanistic model provides a framework for the mathematical abstraction of these complex interactions and for understanding the system as a whole.

Fig. 5 shows a schematic of the model. In short, inhibitory and excitatory neuron inputs undergo low-pass filtering before reaching an *adaptive combiner* [76, 75], forming the neuron’s core. Consistent with Gray’s rules [21, 49, 67, 24], the inhibitory inputs have fixed weights and are collectively represented as $y(t)$. In contrast, the excitatory inputs $x_k(t)$ have adjustable weights w_k , subject to a learning rule. The neuron’s membrane potential represents the adaptive combiner output $z(t)$, subsequently converted to an output spike train with spike rate $\varphi[z(t)]$, where φ is a soft-threshold activation function.

Contrasted with the basic neuron model introduced in Sect. 1.2, this model embodies three distinct new features: *time-variable inputs and outputs*, *non-negativity of weights*, and *plasticity*. Each enhancement notably amplifies the neuron’s computational capabilities, with deeper explorations provided in the subsections below.

3.2 Time-variable inputs and outputs

Whereas we previously assumed slowly changing inputs enabling a pseudo-static approach, we now allow inputs to be vectors of *wavelets*—short, time-variable functions [43]. This assumption mandates a fully dynamic approach, which we detail in this section.

When the inputs enter the synapses, they pass through a battery of low-pass filters with diverse time constants. While summed in the proximal compartment (proximal dendrites and soma), they undergo additional low-pass filtering with the membrane time constant τ_m . In the frequency (Laplace) domain, the transfer function becomes

$$\tilde{z}(s) = \frac{1}{s + 1/\tau_m} [\tilde{\mathbf{w}}^T(s) \tilde{\mathbf{x}}(s) - \tilde{y}(s)],$$

where z is the adaptive combiner output, \mathbf{w} is the vector of excitatory synapse weights, and \mathbf{x} and y are the filtered excitatory and inhibitory inputs, respectively.

The formula above neither includes a factor in front of y nor any representation of the input low-pass filters because we are only interested in invariants under convolution

by fixed matrices. Accordingly, a neuron population acts as an *operator* in the Hilbert space L_2^n , mapping functions to functions. The low-pass filter characteristics render these operators *compact*, meaning we can take advantage of the intuition from matrix multiplication. This is because a compact operator in Hilbert space can be expressed as a matrix multiplication, according to the spectral theorem of operator theory [23], concretized by the Laplace-transformation. The application of the adaptive combiner as a message filter, expressed as convolution in the time domain, corresponds to matrix multiplication in the frequency domain.

An intuitive way to think of going from \mathbb{R}^n to L_2^n is to imagine using piece-wise constant vectors, but separately for each frequency. In this context, diagrams like Fig. 3 pertain to a *specific frequency*.

The following example illustrates the treatment of signals as Hilbert space elements:

Example 1 (*Neuron inputs as points in Hilbert space*). Let's assume that we have a neuron receiving the inhibitory input $y = \cos \omega t + 2 \sin \omega t$ for a short duration. Note that y is a "point" (element) in the Hilbert space L_2 . Excitatory inputs $\mathbf{x} = (\cos \omega t, \sin \omega t)^T$ can also be seen as a point, this time in L_2^2 . (In analogy with the homeostatic function of biological neurons, we remove zero offsets from the inputs, so the signals are always zero-mean.) The neuron will try to adjust \mathbf{w} so that $\mathbf{w}^T \mathbf{x} \approx y$. In this case, the optimal \mathbf{w} is $(1, 2)^T$. \square

Unless otherwise mentioned, we assume that the weight updates are slow compared to the feed-forward operation and that the activation function operates in the linear range (Fig. 4), so we can describe the neuron in the time domain and general time-variable case to within a constant factor by the equation

$$z(t + \Delta t) = \lambda [\mathbf{w}^T \mathbf{x}(t) - y(t)] + (1 - \lambda)z(t) + O(\Delta t^2), \quad (4)$$

where $\lambda = 1 - \exp(-\Delta t / \tau_m)$.

3.3 Non-negative weights

The biological representation of weights as counts of synaptic AMPA receptors [46] inherently implies non-negativity. This fundamental property suggests invariance specifically under *multiplication by non-negative matrices*, indicating *convex cones* as the principal invariant (Fig. 6). Thus, the resulting foundational mathematical framework is an algebra of convex cones in Hilbert space. At first glance, this may seem like a restriction compared to the earlier algebra of subspaces. However, this formulation not only powerfully generalizes but is surprisingly similar to the algebra of subspaces, as will be elaborated upon in Sect. 4.

Example 2 (*Non-negative weights*). The weight vector \mathbf{w} corresponding to the inhibitory input $y = \cos \omega t - 2 \sin \omega t$ and excitatory inputs $\mathbf{x} = (\cos \omega t, \sin \omega t)^T$ is $(1, 0)^T$ instead of $(1, -2)^T$, because weights cannot be negative. \square

3.4 Plasticity

The neuron updates the excitatory weights \mathbf{w} using a built-in adaptive combiner. Such a neuron model, ADALINE for ADaptive LInear NEuron, was first proposed by Widrow

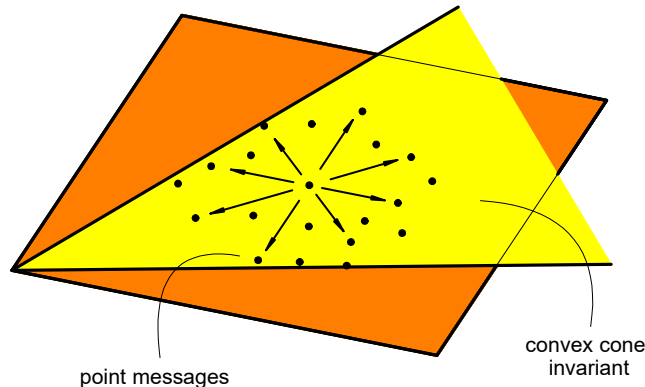


Figure 6: **Convex cone invariants.** When the weight matrix is non-negative, subspaces generalize to convex cones. This representation substantially improves the expressional power of the invariants.

and Hoff [75] based on an adaptive *linear* combiner using the *LMS learning rule* [75]

$$w_k := w_k - \varepsilon x_k z. \quad (5)$$

where $\varepsilon > 0$ is a small learning factor. The name is appropriate because the adaptive linear combiner attempts to adjust a linear combination of input signals to match a desired response signal. At the time, it was difficult to explain mechanistically how the neuron could implement such a mechanism because little was known about the internals of neurons. It was assumed that the mechanism used external feedback, but such feedback would be too slow for biological neurons. ADALINE was abandoned as a neuron model, but under the abbreviation's new interpretation "ADaptive LINear Element" became the basis for the explosive and highly successful development of adaptive filters in signal processing [76, 25, 63].

However, it was recently shown for the present mechanistic neuron model that sufficiently fast internal feedback does exist [46], and that neurons implement an adaptive *conical* combiner using the modified LMS learning rule

$$w_k := \max(0, w_k - \varepsilon x_k z), \quad (6)$$

which ensures the non-negativity of synaptic weights.

While the input low-pass filters are neither orthogonal nor linearly independent, by their diversity, they express an exponential family of functions, which is complete in the sense that a conical combination can approximate any function y in L_2 arbitrarily well provided that the set of excitatory inputs is sufficiently rich. Therefore, in principle, the neuron model can implement any required linear filter characteristic.

The adaptive combiner can be viewed as a device performing a wavelet transform [12, 43]. Its adjusted weights express the inhibitory input as a conical combination of the excitatory inputs.

Example 3 (Plasticity). Continuing example 1, now with the inhibitory input $y = \cos \omega t + 2 \sin \omega t + 3 \cos 3\omega t$ and the excitatory inputs $\mathbf{x} = (\cos \omega t, \sin \omega t)^T$, where the latter can be seen as a *basis* or *frame* of wavelets, the neuron's job is to adjust its

synaptic weights \mathbf{w} to minimize $\|\mathbf{w}^T \mathbf{x} - y\|$. This is performed by the neuron's adaptive filter function effectively projecting y on \mathbf{x} . As in example 1, $\mathbf{w} = (1, 2)^T$, but note that there is a residue $\mathbf{w}^T \mathbf{x} - y = 3 \cos 3\omega t$ because \mathbf{x} is incomplete. Compactly expressed, \mathbf{w} are non-negative wavelet coefficients of y w.r.t. the frame \mathbf{x} . They are not necessarily unique. \square

3.5 Performance and stability of adaptive combiners

The LMS-rule's performance and stability have been extensively scrutinized, yet a direct method for its analysis still needs to be discovered. The rule's inherent non-linearity complicates such evaluations. Nonetheless, as observed by Haykin [25], our grasp of its performance is still robust, even if we might never attain a direct analysis.

The theory of adaptive filters is comprehensive. However, it is straightforward to understand the adaptive combiner's operation informally, *e.g.*, as presented in Sect. 3.6.

Beyond the adaptive linear combiner's objective, the adaptive conical combiner adds the constraint that all weights w_k must be non-negative. This problem subsumes the adaptive linear combiner because by adding inputs $x_{n+k} = -x_k$ and weights $w_{n+k} \geq 0$ to the adaptive conical combiner, it emulates the adaptive linear combiner with its k th weight equal to $w_k - w_{n+k}$. Therefore, analyzing the performance and stability of the adaptive conical combiner is at least as complex as analyzing the adaptive linear combiner. Despite these complexities, we note that both adaptive combiners seen as optimization problems are convex. We can construe their respective update rules as internal-point stochastic steepest gradient descent (SGD) methods, which estimate the gradient based on the most recent inputs.

3.6 * Intuition behind the learning rule

The weight updates are performed discrete times t_p , $p = 1, 2, \dots$, and are best understood in the time domain. Let us assume that the input changes slowly between these sampling points, allowing us to formulate the inputs as discrete processes $X = \{x_p\}_{p=1}^{\infty}$ and $Y = \{y_p\}_{p=1}^{\infty}$. We want to approximate Y by a multiple αX . If we introduce a shorthand for finite sequences by $\mathbf{x} = (x_1, \dots, x_p)$ and similarly for \mathbf{y} , for given p and α , we want to minimize $|\alpha \mathbf{x} - \mathbf{y}|$ while continuously receiving additional x and y components. The optimal α is given by

$$\alpha = \frac{\langle \mathbf{x} | \mathbf{y} \rangle}{\langle \mathbf{x} | \mathbf{x} \rangle},$$

as is well known. Assuming we do not save all the old values $x_j, y_j, j < p$, we must approximate the inner products. If we rewrite

$$\alpha_p = \alpha_{p-1} - \alpha_{p-1} \frac{\langle \mathbf{x} | \mathbf{x} \rangle}{\langle \mathbf{x} | \mathbf{x} \rangle} + \frac{\langle \mathbf{x} | \mathbf{y} \rangle}{\langle \mathbf{x} | \mathbf{x} \rangle} = \alpha_{p-1} - \frac{\langle \mathbf{x} | \alpha_{p-1} \mathbf{x} - \mathbf{y} \rangle}{\langle \mathbf{x} | \mathbf{x} \rangle}$$

and introduce a *forget* or *decay factor* $\lambda \in [0, 1]$ to reduce the weight of old data in the inner product approximations

$$\begin{aligned} s_{xy} &:= \lambda x_p (\alpha_{p-1} x_p - y_p) + (1 - \lambda) s_{xy}, \\ s_{xx} &:= \lambda x_p^2 + (1 - \lambda) s_{xx}, \end{aligned}$$

we can compute

$$\alpha_p \approx \alpha_{p-1} - \frac{s_{xy}}{s_{xx}}.$$

Introduction of a small learning factor $\varepsilon > 0$ improves the stability of the algorithm at the cost of convergence speed,

$$\alpha := \alpha - \varepsilon \frac{s_{xy}}{s_{xx}}.$$

With $\lambda = 1$, this is essentially the LMS-rule, or more specifically, a variation known as the normalized LMS-rule (NLMS). Having $\lambda < 1$ corresponds to low-pass filtering the adaptive combiner output.

3.7 Abstract model of populations

The generalization to a population of m neurons is straightforward. We have m -dimensional vectors \mathbf{y} and \mathbf{z} of inhibitory inputs and outputs, respectively. As before, we have an n -dimensional vector \mathbf{x} of excitatory input.

Example 4 (Populations). Now we expand examples 1 and 3 to a two-neuron population ($m = 2$). If the population first receives the inhibitory and excitatory inputs

$$\begin{aligned}\mathbf{y}^{(1)} &= (\cos \omega t + 2 \sin \omega t + 3 \cos 3\omega t, 4 \cos \omega t)^T \in L_2^2, \\ \mathbf{x}^{(1)} &= (\cos \omega t, \sin \omega t, 0, 0)^T \in L_2^4,\end{aligned}$$

the neuron develops the weight matrix

$$W = \begin{pmatrix} 1 & 2 & ? & ? \\ 4 & 0 & ? & ? \end{pmatrix}^T,$$

where '??' denotes an indefinite value. Subsequently, if the population receives a second message

$$\begin{aligned}\mathbf{y}^{(2)} &= (5 \cos 2\omega t, 6 \sin 2\omega t)^T \in L_2^2, \\ \mathbf{x}^{(2)} &= (0, 0, \cos 2\omega t, \sin 2\omega t)^T \in L_2^4,\end{aligned}$$

the weight matrix adapts to

$$W = \begin{pmatrix} 1 & 2 & 5 & 0 \\ 4 & 0 & 0 & 6 \end{pmatrix}^T.$$

The set of two message points or vectors $\{\mathbf{y}^{(1)}, \mathbf{y}^{(2)}\}$ constitutes a basis or frame for a cone in L_2^2 . We can say that the neuron has learnt the matrix W which encodes the translation of the cone from \mathbf{x} -space to \mathbf{y} -space by the two examples $(\mathbf{y}^{(1)}, \mathbf{x}^{(1)})$ and $(\mathbf{y}^{(2)}, \mathbf{x}^{(2)})$. Note that any conical combination $\alpha \mathbf{x}^{(1)} + \beta \mathbf{x}^{(2)}$, where $\alpha, \beta \geq 0$, is appropriately translated by the same W . \square

The population output \mathbf{z} is updated as (cf. (4))

$$\mathbf{z} := \lambda (W^T \mathbf{x} - \mathbf{y}) + (1 - \lambda) \mathbf{z}, \quad (7)$$

where the update rule for the weight matrix W in the time domain is

$$W := W - \varepsilon \mathbf{x} \mathbf{z}^T$$

for the linear combiner and

$$W := \max(0, W - \varepsilon \mathbf{x} \mathbf{z}^T)$$

for the conical combiner, where $\max(\cdot)$ is applied component-wise.

For the subspace case with $\lambda = 1$, suppose that the components of \mathbf{y} in (7) are independent and identically distributed Gaussian and that $\mathbf{x} = B\mathbf{y}$, where B is a fixed matrix. It is well known that the minimum of the expectation $E[|\mathbf{z}|] = E[|W^T\mathbf{x} - \mathbf{y}|]$ occurs for

$$W^T = B^+ + \Phi(BB^+ - I),$$

where Φ is an arbitrary matrix in $\mathbb{R}^{m \times n}$. Here, W does not converge *strongly* because of the additional term $\Phi(BB^+ - I)$, but it does converge *weakly* because $W^T\mathbf{x} - \mathbf{y}$ approaches

$$[B^+ + \Phi(BB^+ - I)]B\mathbf{y} - \mathbf{y} = (B^+B - I)\mathbf{y}$$

independently of Φ . If we think of $\mathbf{x}, \mathbf{y}, \mathbf{z}$ as samples from the subspaces q, p, r , respectively, we can express this relation by the rejection of p from q ,

$$r = p \neg q. \quad (8)$$

To the best of the author's knowledge, there is no explicit formula for an optimal W in the conical case, but as we shall see in Sect. 5.1, there is a generalization of (8) to convex cones.

4 The algebra of convex cones

In this section, we investigate the basic mathematical properties of convex cones and the operations in an algebra of such objects. We postpone the issue of implementation by biological neurons until Sect. 5.

4.1 Finite convex cones

Formally, we define a *finite convex cone* as the set of conical combinations $\sum_k \lambda_k \mathbf{v}_k$, where the λ_k are non-negative real numbers and the vectors \mathbf{v}_k belong to a *finite* subset of real Hilbert space H termed a *frame* for a . The frame vectors can be visualized as the ribs of an umbrella with the cap at the origin, or as the flowers in a bouquet. Although general convex cones are proper invariants, finiteness is convenient in the study for practical purposes such as representation and computer implementation, where a finite set of vectors suffice to represent the cone, and we can apply induction over frames for proofs.

4.2 Basic operations on convex cones

We will generalize the five basic operations *complement*, *sum*, *intersection*, *projection*, and *rejection* from the algebra of subspaces in Sect. 2 (Fig. 7). The non-negativity of weights mandates one new operation, *reflection* (unary ' \neg '), which we give the same precedence order as ' $+$ '.

4.2.1 Dual

The *dual* $\neg a$ of a cone a generalizes the *complement* operation and is the set of all vectors forming a right or obtuse angle with all vectors in a :

$$\neg a \triangleq \{\mathbf{v} \in H \mid \forall \mathbf{u} \in a : \langle \mathbf{v}, \mathbf{u} \rangle \leq 0\}.$$

4.2.2 Sum

Sum is the conic hull of two convex cones. We write the sum of two cones a and b as

$$a + b \triangleq \{\mathbf{v} \in H \mid \exists \mathbf{u} \in a, \mathbf{w} \in b : \mathbf{v} = \mathbf{u} + \mathbf{w}\}.$$

The *conic hull* $\text{Conic}(c)$ of a *non-convex* cone c can be defined as the sum of c with itself, $\text{Conic}(c) \triangleq c + c + \dots + c$ (m times) $= \Sigma_{i=1}^m c$, where m is the size of some frame for c .

4.2.3 Conic projection

The orthogonal projection of a point x on a closed convex cone is the point in the cone nearest to x . Such a point always exists and is unique according to the projection theorem (Sect. 4.4.1). The orthogonal projection of a cone a on another cone b is a cone but not necessarily convex. An example is when a and b are disjoint except for the apex, and the projection of a on b is limited to the boundary of b . We extend the projection to its conic hull and name it *conic projection* to guarantee a convex result,

$$a \perp b \triangleq \text{Conic}\{\mathbf{v} \in b \mid \exists \mathbf{u} \in a : \mathbf{v} = \arg \min_{\mathbf{w} \in b} |\mathbf{u} - \mathbf{w}|\}.$$

Unless stated otherwise, when we write *projection* of a cone below, we mean *conic projection*. When referring to the original, non-extended projection, we prefix by “orthogonal”.

4.2.4 Conic rejection

We define *conic rejection* of b from a as the *conic projection* of a on the *dual* of b ,

$$a \neg b \triangleq \text{Conic}\{\mathbf{v} \in \neg b \mid \exists \mathbf{u} \in a : \mathbf{v} = \arg \min_{\mathbf{w} \in \neg b} |\mathbf{u} - \mathbf{w}|\}.$$

We can also write this as

$$a \neg b = a \perp (\neg b). \quad (9)$$

Conic projection can be expressed as two *conic rejections* (Sect. 4.4.2),

$$a \perp b = a \neg (a \neg b). \quad (10)$$

4.2.5 Intersection

The *intersection* of two convex cones is trivially

$$a \cap b \triangleq \{\mathbf{v} \in a \cap b\}.$$

It can be expressed as a combination of three *conic rejections* and two *sums* (Sect. 4.4.3):

$$a \cap b = a \neg (b \neg a + a \neg b) \quad (11)$$

$$= b \neg (b \neg a + a \neg b) \quad (12)$$

$$= (a + b) \neg (b \neg a + a \neg b). \quad (13)$$

4.2.6 Reflection

Reflection mirrors a cone through the origin. This operation is trivial for subspaces because a subspace containing a vector \mathbf{v} always contains $-\mathbf{v}$, but it is a meaningful operation for cones. It is defined simply as

$$-a \triangleq \{-\mathbf{v} \mid \mathbf{v} \in a\}.$$

The *reflection of the dual* $-(\neg a)$ is the *polar cone*, but some authors use the opposite naming. The *linear hull* \bar{a} of a cone a equals the *sum* of a and its reflection,

$$\bar{a} \triangleq a + (-a).$$

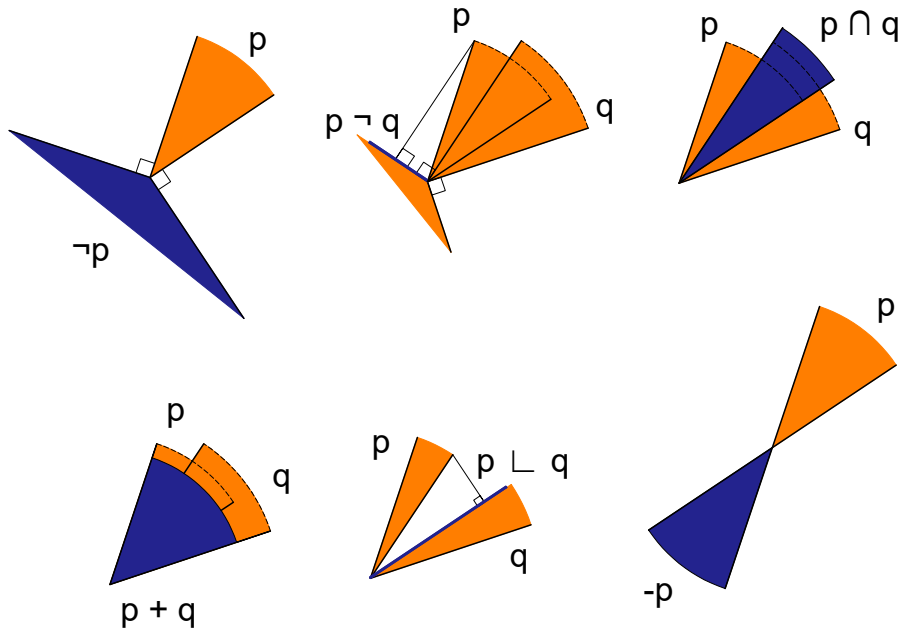


Figure 7: *Basic operations on convex cones.* Because cones are invariants under multiplication with non-negative matrices, the *reflection* operation is needed. The other operations are generalizations of subspace operations.

Example 5 (*Operations on cones*). Continuing example 4, with the inputs and the weight matrix

$$\begin{aligned} \mathbf{y}^{(1)} &= (\cos \omega t + 2 \sin \omega t + 3 \cos 3\omega t, 4 \cos \omega t)^T, \\ \mathbf{x}^{(1)} &= (\cos \omega t, \sin \omega t, 0, 0)^T, \\ \mathbf{y}^{(2)} &= (5 \cos 2\omega t, 6 \sin 2\omega t)^T, \\ \mathbf{x}^{(2)} &= (0, 0, \cos 2\omega t, \sin 2\omega t)^T, \\ W &= \begin{pmatrix} 1 & 2 & 5 & 0 \\ 4 & 0 & 0 & 6 \end{pmatrix}^T, \end{aligned}$$

we find that the result of the first message is

$$\mathbf{z}^{(1)} = W^T \mathbf{x}^{(1)} - \mathbf{y}^{(1)} = (-3 \cos 3\omega t, 0)^T$$

and likewise, the result of the second message is

$$\mathbf{z}^{(2)} = (0, 0)^T = \mathbf{0}.$$

The result is the convex cone Z having the frame $\{\mathbf{z}^{(1)}\}$, which is the reflected rejection of the cone X having the frame $\{\mathbf{x}^{(1)}, \mathbf{x}^{(2)}\}$ from the cone Y having the frame $\{\mathbf{y}^{(1)}, \mathbf{y}^{(2)}\}$. \square

4.3 Relations between convex cones

We use the same definition of *emptiness* as for subspaces in Sect. 2.4, namely, being equal to $\{\mathbf{0}\}$.

An essential advantage of convex cones over subspaces is that a *partial order* can be defined between cones even if they have the same linear hull, enabling a more nuanced comparison. We define $p \preceq q$ as equivalent to $p \subseteq q$. Testing is straight-forwardly performed by *conic rejection*: A convex cone p is a subset of another convex cone q if and only if $p \neg q$ is empty.

Cones a and b can be compared by computing the rejections $a \neg b$ and $b \neg a$. If $a \neg b$ is empty, then $a \subseteq b$; if $b \neg a$ is empty, then $b \subseteq a$; if both are empty, $a = b$.

One possible graded comparison of finite convex cones a and b is by computing

$$\begin{aligned} \cos \theta &= \min \left(\inf_{\mathbf{x} \in a, \mathbf{y} \in a \perp b} \frac{\langle \mathbf{x}, \mathbf{y} \rangle}{\|\mathbf{x}\| \|\mathbf{y}\|}, \inf_{\mathbf{x} \in b, \mathbf{y} \in b \perp a} \frac{\langle \mathbf{x}, \mathbf{y} \rangle}{\|\mathbf{x}\| \|\mathbf{y}\|} \right) \\ &\approx \min \left(\inf_{\mathbf{x} \in F_a} \sup_{\mathbf{y} \in F_b} \frac{\langle \mathbf{x}, \mathbf{y} \rangle}{\|\mathbf{x}\| \|\mathbf{y}\|}, \inf_{\mathbf{x} \in F_b} \sup_{\mathbf{y} \in F_a} \frac{\langle \mathbf{x}, \mathbf{y} \rangle}{\|\mathbf{x}\| \|\mathbf{y}\|} \right), \end{aligned}$$

where F_c denotes a frame of cone c . The smaller $\cos \theta$, the more different the cones.

4.4 * Properties of the algebra of convex cones

4.4.1 Some well-known properties of convex cones

The following projection theorem is fundamental for convex cones [26, 39]: *Let b be a closed convex cone and $\mathbf{x} \in H$. Then there is a unique $\mathbf{y} \in b$ and a unique $\mathbf{z} \in \neg b$ such that $\mathbf{x} = \mathbf{y} + \mathbf{z}$ and $\langle \mathbf{y}, \mathbf{z} \rangle = 0$ (Fig. 8). \mathbf{y} is the nearest point of b to \mathbf{x} and \mathbf{z} is the nearest point of $\neg b$ to \mathbf{x} . Furthermore, a necessary and sufficient condition that \mathbf{y} be unique is that $\langle \mathbf{x} - \mathbf{y}, \mathbf{w} - \mathbf{y} \rangle \leq 0$ for all $\mathbf{w} \in b$, and similarly for \mathbf{z} .*

Many other useful properties of convex cones exist [22, 26],

$$a \perp b \subseteq b, \tag{14}$$

$$a \subseteq b \Leftrightarrow \neg a \supseteq \neg b, \tag{15}$$

$$a = \neg \neg a, \tag{16}$$

$$a \perp (a \perp b) = a \perp b \tag{17}$$

$$a \cap b = \neg(\neg a + \neg b). \tag{18}$$

Below, we present two additional essential relations.

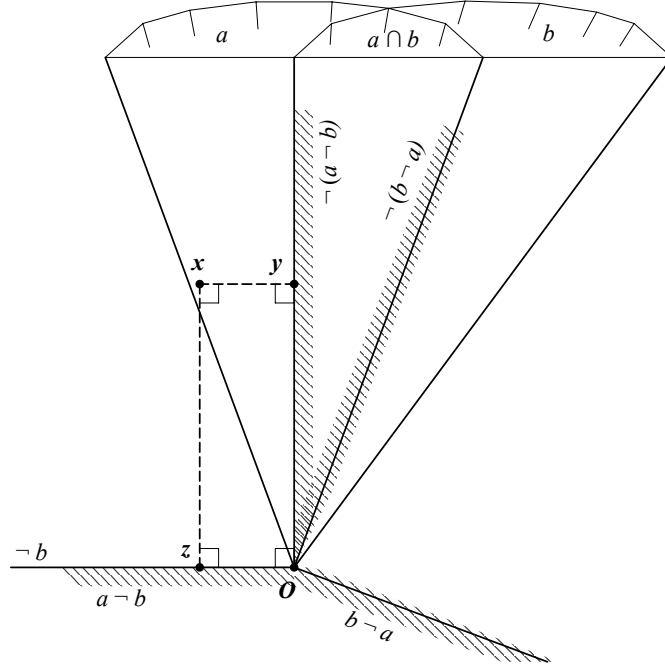


Figure 8: *Cross-section of two intersecting cones.* Two intersecting cones a and b along the 2D cross-section containing the position vector $\mathbf{x} \in a$ and its projections \mathbf{y} and \mathbf{z} on b and $\neg b$, respectively. The hashed areas show projections of the annotated cones near the boundaries.

4.4.2 Conic projection by conic rejections

Consider the projection \mathbf{y} of a point \mathbf{x} in a cone a on another cone b . Let the projection of \mathbf{x} on the dual $\neg b$ be \mathbf{z} . The rectangle $O\mathbf{y}\mathbf{x}\mathbf{z}$ defines a two-dimensional cross-section (Fig. 8). A roundabout way of projecting \mathbf{x} on b is to first project a on the dual $\neg b$, and then project \mathbf{x} on the dual of this dual. Although $c = \neg(a \neg b)$ may be larger than b ($b \subseteq c$), the convexity of b and c means that the point in b nearest to \mathbf{x} is also the nearest point in c , so

$$a \perp b = a \perp \neg(a \neg b) = a \neg(a \neg b). \quad (19)$$

□

4.4.3 Intersection by conic rejections and sums

Substituting $b \neg a$ and $a \neg b$ for a and b into (18),

$$\neg(b \neg a + a \neg b) = \neg(b \neg a) \cap \neg(a \neg b).$$

Clearly, $b \neg a \subseteq \neg a$, so $\neg(b \neg a) \supseteq a$, and similarly $\neg(a \neg b) \supseteq b$, from which

$$\neg(b \neg a) \cap \neg(a \neg b) \supseteq a \cap b. \quad (20)$$

Since $a \cap b \subseteq a$, projecting a on the expression above yields

$$a \perp [\neg(b \neg a) \cap \neg(a \neg b)] \supseteq a \cap b,$$

so

$$a \neg (b \neg a + a \neg b) \supseteq a \cap b.$$

For showing this relation in the other direction, let \mathbf{x} be an element of a and let \mathbf{y} be the projection of \mathbf{x} on $a \cap b$ (Fig. 8). Then

$$\begin{aligned} \mathbf{y} &= \mathbf{x} \lrcorner (b \cap a) \\ &= \mathbf{x} \lrcorner [\neg(a \neg b) \cap a] \\ &= \mathbf{x} \lrcorner [\neg(a \neg b) \cap \neg(b \neg a)] \\ &\in a \cap b, \end{aligned}$$

where we used the convexity of the cones. As a consequence,

$$a \lrcorner [\neg(b \neg a) \cap \neg(a \neg b)] \subseteq a \cap b,$$

implying that

$$a \neg (b \neg a + a \neg b) = a \cap b.$$

Analogously, we find that

$$a \cap b = b \neg (b \neg a + a \neg b)$$

and

$$a \cap b = (a + b) \neg (b \neg a + a \neg b).$$

□

4.5 * Invariance of the algebra of convex cones

To demonstrate the invariance of the algebra of convex cones somewhat more formally, assume that M is a non-negative matrix. For a convex cone a , let Ma denote the set

$$Ma = \{M\mathbf{v} \mid \mathbf{v} \in a\} = \{\mathbf{v} \mid \mathbf{v} \in Ma\},$$

which is also a convex cone because a frame for Ma is a conical combination of frame vectors for a .

We first need to show that for cones a and b , $M(-a) = -Ma$ and $M(a + b) = Ma + Mb$. We have

$$M(-a) = \{M(-\mathbf{v}) \mid \mathbf{v} \in a\} = \{\mathbf{v} \mid \mathbf{v} \in -Ma\} = -Ma$$

and

$$\begin{aligned} M(a + b) &= \{\mathbf{v} \in H \mid \exists \mathbf{u} \in a, \mathbf{w} \in b : \mathbf{v} = M(\mathbf{u} + \mathbf{w})\} \\ &= \{\mathbf{v} \in H \mid \exists \mathbf{u} \in Ma, \mathbf{w} \in Mb : \mathbf{v} = \mathbf{u} + \mathbf{w}\} \\ &= Ma + Mb. \end{aligned}$$

We also need to show that $M(\neg a) = \neg M(a)$. Here, we require M to have a sparse structure (cf. Sect. 2.5) that retains the inner product's sign, $\text{sign}\langle \mathbf{x}, \mathbf{y} \rangle = \text{sign}\langle M\mathbf{x}, M\mathbf{y} \rangle$.

$$\begin{aligned} M(\neg a) &= \{M\mathbf{v} \in H \mid \forall \mathbf{u} \in a : \langle \mathbf{v}, \mathbf{u} \rangle \leq 0\} \\ &= \{\mathbf{v} \in H \mid \forall \mathbf{u} \in a : \langle M\mathbf{v}, M\mathbf{u} \rangle \leq 0\} \\ &= \{\mathbf{v} \in H \mid \forall \mathbf{u} \in Ma : \langle \mathbf{v}, \mathbf{u} \rangle \leq 0\} \\ &= \neg Ma. \end{aligned}$$

Suppose that \mathbf{y} is the projection of an \mathbf{x} in cone a on the convex cone b . According to the projection theorem (Sect. 4.4.1), $\langle \mathbf{x} - \mathbf{y}, \mathbf{w} - \mathbf{y} \rangle \leq 0$ for all $\mathbf{w} \in b$. This implies that $\langle M\mathbf{x} - M\mathbf{y}, \mathbf{w} - M\mathbf{y} \rangle \leq 0$ for all $\mathbf{w} \in Mb$, meaning that $M\mathbf{y}$ must be the projection of $M\mathbf{x}$ on cone Mb , and as a consequence, $M(a \perp b) = Ma \perp Mb$.

Finally, $M(a \neg b) = Ma \neg Mb$ and $M(a \cap b) = Ma \cap Mb$ follow from (9) and (13), respectively. \square

5 Neuronal implementation of computation

This section explores how neuron populations act as computational operators in the algebra of convex cones. It becomes evident that populations are qualitatively more potent than individual neurons. We assume that weights have settled (converged weakly), ensuring stable outputs.

5.1 The neuron population as a primitive operator

A sequence of messages transmits a cone along an axon bundle. The axons define coordinate axes, whereas the messages outline the cone via correlations between axon signals or point densities (Fig. 6). The non-negativity of a population's weight matrix guarantees that the cone remains a cone after multiplication by the matrix or traversing the population. It is worth noticing that this representation is robust against mixing up different cones because even if some of the messages collide, much of the entire sequences must match (correlate) to risk confusion. If two correlated inputs weaken proportionately, the message points will move along a ray from the origin, but the cone is insensitive to such variations.

The matrix W of synaptic weights functions as memory. The weights are updated stepwise by the learning rule (6), where the learning rate ε determines the convergence speed. A population stores a convex cone p , represented by a sequence of inhibitory input messages \mathbf{y} , by gradually adapting the weights W so that the sequence of products $W^T \mathbf{x}$ approximates p , where \mathbf{x} denotes an excitatory input message. This sequence of products represents the *conic projection* $p \perp q$ of the inhibitory input cone p on the excitatory input cone q . The conic projection is then conically rejected from p and subsequently output as $-[p \neg (p \perp q)] = -(p \neg q)$. The *reflection* derives from p being inhibitory, requiring a sign change.

In summary, the generic neuron population in Fig. 5 representing the fundamental primitive and having the defining equation (4) can be written

$$r = -(p \neg q),$$

where r , p , and q denote the output cone, the inhibitory input cone, the excitatory input cone, respectively.

The neuron population serves as a *primitive operator* because all basic operations except *dual* can be expressed through this operator, as detailed below. While *dual* is not implementable by populations because it would violate the sparsity constraint (Sect. 1.5), its intended effect can usually be achieved by *conic rejection* (Sect. 4.4.3).

5.2 Basic operations in terms of primitive operators

A mere zero to four neuron populations are adequate to carry out the basic operations of the algebra of convex cones. The basis for the circuits is the formula collection pro-

vided in Sect. 4.2, its depiction in Fig. 9, and elaboration below. The figure presents generic populations as rounded triangles, distinguishing inhibitory and excitatory inputs with '-' and '+' symbols, respectively. The flow of signals progresses from left to right.

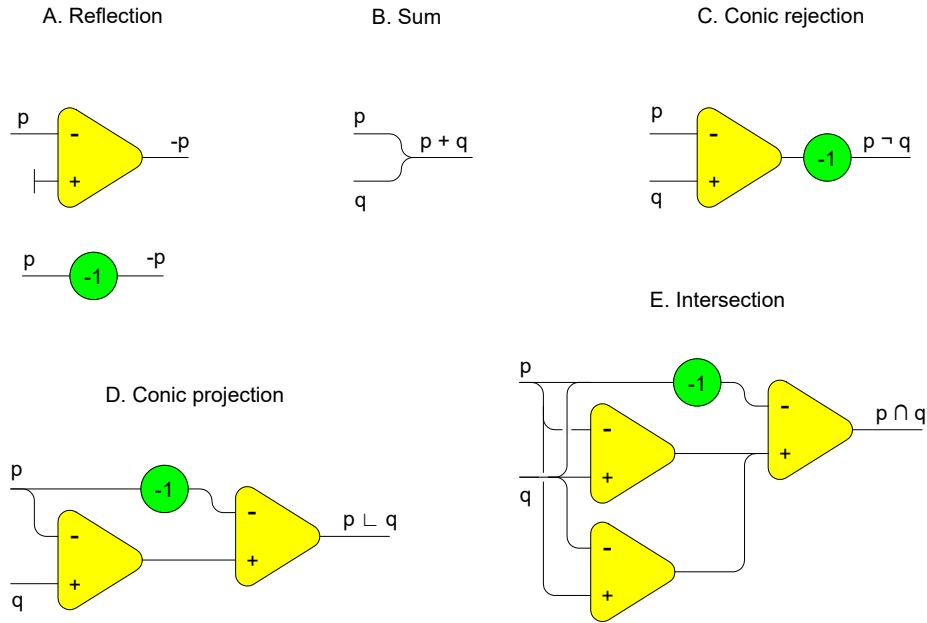


Figure 9: **Basic operations as implemented by neuron populations.** Populations can implement all basic operations except *dual*. For convenience, we introduce a shorthand symbol for *reflection* (A, bottom).

Reflection: A single generic neuron population can implement the *reflection* operation without excitatory inputs (Fig. 9 A, top), but for brevity, we dedicate a symbol to this function: the encircled ‘-1’ (Fig. 9 A, bottom). It has a biological counterpart in local inhibitory neurons ubiquitous in the CNS. An obvious but helpful rule for minimizing the number of reflections in a circuit is

$$-(y \neg x) = (-y) \neg (-x). \quad (21)$$

Sum: *Sum* does not require any populations but is achieved by simply bundling together the axons (Fig. 9 B).

Conic rejection: *Conic rejection* is the “native” operation of the neuron population, but needs an appended *reflection* to specify the sign change of the inhibitory input (Fig. 9 C).

Conic projection: A combination of three populations, one of which is a *reflection*, can implement *conic projection* using relation (10) and (21) (Fig. 9 D).

Intersection: *Intersection* has the most complex implementation. It can be realized by three *conic rejections* and one *reflection*, using relations (13) and (21) (Fig. 9 E).

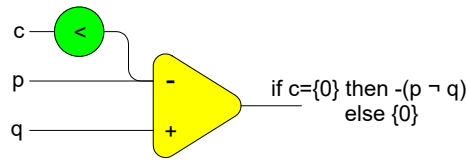


Figure 10: **Conditionals.** By an additional, strong inhibitory input, populations can implement conditionals.

5.3 Conditionals

Neuron populations can execute conditionals through potent inhibitory input (Fig. 10), forcing the neuron into the activation function’s *cutoff* range. In this illustration, the circle labeled with a “<” symbol indicates a population capable of producing the blocking signal. Basket cells [44] are biological analogs to such populations. The function implemented is

$$\text{if } c = \{0\} \text{ then } [-(p - q)] \text{ else } \{0\}.$$

5.4 Memory operations

We have already described the primary *memory write* operation as synaptic weight updates of the neuron population in Sect. 5.1.

Any feed-forward action can be treated as a *memory read* because any excitatory input reads the weight matrix and multiplies it with the input message. A more distinct memory read is achieved by momentarily keeping the inhibitory input \mathbf{y} inactive while sending excitatory messages \mathbf{x} to the population. This produces the outputs $W^T \mathbf{x} - \mathbf{y} = W^T \mathbf{x}$, which equates to $p \perp q$.

When writing memory, the inhibitory input p works as the contents and the excitatory input q works as the address or lookup key. Upon readout, an exact match with q is not required. The combination of sparsity and a soft-threshold activation function allows associative lookup [35, 53].

5.5 Adaptive filter applications

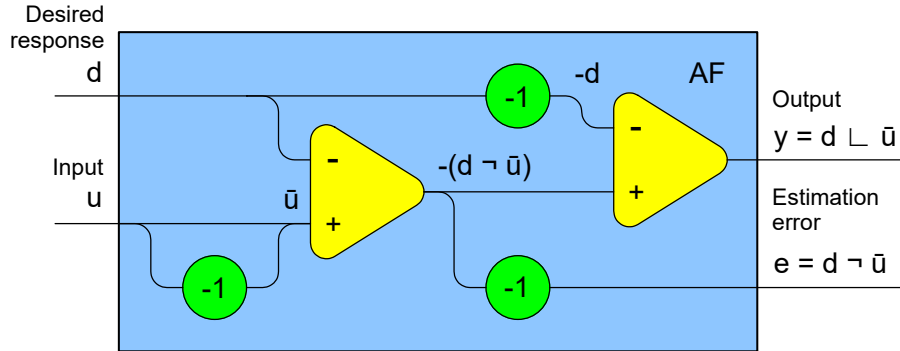
The classical adaptive filter is a workhorse of statistical signal processing [25, 63, 76]. It has a main input u , a desired response input d , a main output y , and an estimation error output e . In our notation, the main output is the projection $d \perp \bar{u}$, and the error output is the rejection $d \neg \bar{u}$. An adaptive filter comprises two generic neuron populations and three local inhibitory populations (Fig. 11, top).

The versatility of the adaptive filter originates in its capability to perform many different functions depending on its connections. Applications can be divided into four classes (Fig. 11):

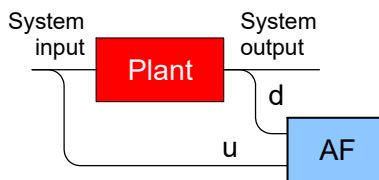
I. Identification: In this class, the adaptive filter establishes a linear model that aligns best with an unfamiliar system, termed the “plant”. It aims to identify and mirror the behavior of this unknown system.

II. Inverse Modeling: Here, the adaptive filter’s role is essentially flipped. Instead of modeling the plant directly, the filter offers an inverse representation of the system. It aims to reverse the behavior of the plant, providing a model that can counteract or undo the effects of the original system.

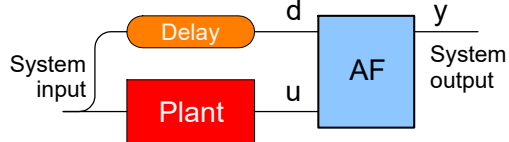
Classical adaptive filter (AF) by neuron populations



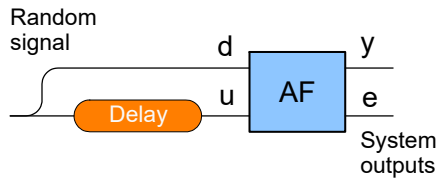
I. Identification



II. Inverse modelling



III. Prediction



IV. Noise cancelling

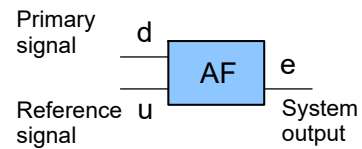


Figure 11: **Classical adaptive filter applications by neuron populations.** Neuron populations can build a classical adaptive filter with projection output y and error output e . In this configuration, neuron populations can directly realize the adaptive filter application classes I-IV [25]. “Plant” refers to an unknown transfer function.

III. Prediction: Within this class, the adaptive filter’s primary objective is to forecast a random signal or even anticipate the prediction error itself. Analyzing past data can project future values or the discrepancy in such predictions.

IV. Noise Cancelling: For this class, the adaptive filter processes a primary signal contaminated with an interference signal. Alongside, it receives a reference signal which carries data about the noise disturbances. The adaptive filter’s output is the cleaned primary signal where the interference has been nullified or substantially reduced.

6 Results

Starting from a non-speculative, strictly mechanistic model of a neuron with plasticity, we developed a mathematical characterization of information processing by neuron populations in the CNS characterizable as an algebra of convex cones in real Hilbert space.

These invariants cannot be extracted from a single vector of instantaneous spike rates but require sequences of such vectors, which express the invariants as convex cones. The invariance remains under convolution by positive fixed compact operators.

Neuron populations can be conceived as operators in the algebra, taking cones as operands and delivering new cones as results. The basic operations on the cones are sum, intersection, reflection, projection, and rejection. Networks of neuron populations can form expressions implementing algebra operations that retain the sparsity of representations. They can also implement conditionals as well as memory read and write operations.

The fact that five neuron populations suffice to fully implement the classical applications of multi-dimensional adaptive filters used in statistical signal processing demonstrates the computational prowess of neuron populations.

7 Discussion

7.1 Interpretation of the invariant and the operations

Our mathematical framework for neuron information processing has been firmly rooted in a mechanistic model, sidestepping speculation. Nevertheless, to shed light on the model's depth, one might liken a message to a "thought" and the cone invariant to a "concept" for a more intuitive grasp.

In abstract terms, we can interpret *sum* as generalization or abstraction; *complement* and *dual* as logical or Boolean negation, or independence; *projection* as specialization or extraction of some relevant property; and *intersection* as logical conjunction. *Rejection* can be interpreted as asymmetric difference or innovation. Moreover, it has an impressive history as a statistical concept tracing back to Wold [77], who proved that every covariance-stationary time series can be written as the sum of two time series, one deterministic and associated with *projection*, and one stochastic and associated with *rejection*. The idea inspired both Wiener and Kolmogorov [25], and Kailath [28] introduced the name *innovation* for the stochastic white-noise process involved. Today, it is foundational in signal processing and control. In neuroscience, the idea of innovation has appeared under many names, including *novelty* [34], *unexpectedness* [5], *prediction error* [64], *decorrelation* [9], *surprise* [16], and *saliency* [69].

To illustrate the basic operations concretely, let us consider the observations of numerous red objects, creating a cone invariant encapsulating the concept of *red*. Perception of a spectrum of colors results in the broader concept of *color*. Intuitively, *projection* can be viewed as the distillation of a specific trait from a concept: projecting *red umbrella* onto *color* extracts *red*. *Sum* acts as generalization: summing *umbrella*, *rain coat*, and *rubber boots* conceptualizes as *rain gear*. Meanwhile, *rejection* of *rain gear* from *red umbrella* leaves us with *red*, demonstrating a logical difference

7.2 Subspaces and algebras of concepts

Representation of knowledge by subspaces has a long history, one of the pioneers being Watanabe [74]. Substantial contributors to subspace methods are Kohonen [34] and Oja [50]. Tsuda [68] considered subspaces of Hilbert space. Early to propose neurons as compact operators in Hilbert space was MacLennan [41], who also realized the significance of overcomplete wavelet frames.

Generally speaking, published work on concept representations is typically not based on mechanistic neuron models but propose high-level theoretical models as hypotheses matching observations in cognitive science.

Algebras of concepts seem to have been considered mostly in the fields of information retrieval and psychology, but generally only as algebras of subspaces [70, 1, 2].

Hyperdimensional computing or vector symbolic architectures reviewed in [30, 31], leverages high-dimensional representations for knowledge processing. Designed for computational efficiency, most draw top-down inspirations from cognitive science. An outlier is Stewart et al. [66], integrating high-dimensional vectors with an empirical spiking neuron model. Our algebra of convex cones is a (matrix) symbolic architecture, but in contrast, is a strictly mechanistic model built bottom-up from the neurobiological properties of neurons.

The algebra of convex cones, detailed in Sect. 4, mirrors the algebra of subspaces in being a topological lattice. Here, the “join” and “meet” operations are embodied by *sum* and *intersection*. However, there is a catch: the sparsity requirement sets a cap on the dimensionality achievable via *sum*. When transposed onto neuron populations, this constraint trims the topological lattice down to a semi-lattice, at most.

Donoho [11] demonstrated that a straightforward weight translation towards zero can efficiently accomplish noise removal and dimension reduction. This technique is remarkably suitable for the adaptive conical combiner’s learning rule, capitalizing on its inherent soft-thresholding trait (6).

7.3 Adaptive filters in neuroscience

Adaptive filters, initially proposed by Widrow and Hoff [75], have become a recurrent theme in neuroscience. Early applications by Kohonen [34] targeted associative memory and related functions [35]. These filters are often employed to model parts of the cerebellum [17, 78, 29, 9].

Notably, some studies have experimentally identified neurons exhibiting behavior akin to Fourier analyzers [57, 10].

7.4 Matrix embeddings

Foundation Models or Large Language Models [80] of current AI-systems use high-dimensional vector embeddings for concept encoding. However, the rudimentary structure of vector spaces limits their representation capacity, for example, when trying to generalize a set of vectors.

A superior alternative is a subspace representation, which offers a *sum* operation. A *matrix embedding* can accomplish this by using a positive semi-definite matrix AA^T derived from the covariance matrix of observations.

The pinnacle of embeddings is achieved through a finite convex cone representation, employing the full non-negative matrix A representing frame vectors. This method

enables a sophisticated partial ordering of concepts, surpassing what is feasible with subspaces, as detailed in Sect. 2.4 and Sect. 4.3.

7.5 Cognitive science aspects

Gärdenfors [20] proposed *conceptual spaces*, a knowledge representation layer bridging the gap between neurobiology and cognition. Despite resting on a neurobiological basis, the algebra of convex cones fits well into this framework. Emphasizing this connection, a subsequent paper on conceptual spaces by Balkenius and Gärdenfors [4] posited that concepts ought to have convex representations.

Research has shown that individuals find it challenging to process sentences containing negations and disjunctions compared to affirmative statements and conjunctions [48, 65]. Our model explains this cognitive quirk because the algebra does not support low-level native representation of negation and disjunction, necessitating higher-level representations for these connectives.

The Gestalt theory presented by Köhler [32] faced criticism due to the absence of a biological rationale. However, the invariant introduced in this paper is founded on robust biological grounds and resonates with Köhler’s notion of a *unit*.

The term *synergy*, prevalent in psychophysics, describes the intrinsic coordination of a large number of degrees of freedom acting in concert [6, 38, 61]. Synergies correspond well to the eigenvectors of the message sequence covariance matrix, the basis vectors of the subspace forming the linear hull of a convex cone.

7.6 A programming language for the brain?

The operations carried out by neuron populations resemble low-level, “assembly”, instructions in a computer, with data represented as convex cones. The set of operations outlined in Sect. 5 is notably potent, enabling sophisticated operations to be accomplished with only a few neuron populations. It raises the intriguing possibility of a higher-level language that can be compiled or interpreted through these operations.

This model introduces the possibility of a neuronal “disassembler”—a tool capable of taking descriptions of population networks and reverse-engineering them to deduce their high-level functions.

It is essential to underline that our discourse primarily encompasses populations of generic neurons. Although representative of numerous CNS neurons, they do not capture all neuronal varieties. Specific neurons exhibit distinctive attributes, possibly adding operations not covered in our discussion.

8 Conclusions

This paper’s main conclusion is that neuron populations in the CNS implement an algebra of invariants, interpretable as convex cones in real Hilbert space.

The unique approach to this conclusion is rooted in a non-speculative strictly mechanistic neuron model with plasticity. Experimental observations underpin every element of the neuron model.

The resulting mathematical structure of data and operations emerges logically from features like invariance, sparsity, plasticity, and activation function properties.

Moreover, a sequence of rate vectors is required to identify an invariant. Matrix (subspace and cone) embeddings have a significant advantage over vector embeddings

in that they can perform generalization as a sum operation. Cones outperform subspaces for defining partial orders and hierarchies. All mathematical structures admit a formulation entirely above the spiking level of abstraction.

While this article does not claim that the CNS necessarily represents concrete cognitive *concepts* as convex cones, it does suggest that neuron populations possess the power to communicate, process, retrieve, and store such invariants. Finding an alternative invariant that is simpler, more effective, and better aligned with observations is a formidable challenge.

Acknowledgments

The author is grateful to Dr. Sverker Janson at RISE for support.

Declaration of competing interests

The author declares that he has no known competing financial interests or personal relationships that could have appeared to influence the work reported in this paper.

References

- [1] Diederik Aerts and Liane Gabora. A theory of concepts and their combinations I. *Kybernetes*, 34(1/2):167–191, January 2005. doi:10.1108/03684920510575799.
- [2] Diederik Aerts and Liane Gabora. A theory of concepts and their combinations II: A Hilbert space representation. *Kybernetes*, 34(2/2):192–221, January 2005. doi:10.1108/03684920510575807.
- [3] Bruno B. Averbeck, Peter E. Latham, and Alexandre Pouget. Neural correlations, population coding and computation. *Nature Rev Neurosci*, 7:358–366, May 2006. doi:10.1038/nrn1888.
- [4] Christian Balkenius and Peter Gärdenfors. Spaces in the brain: From neurons to meanings. *Frontiers in Psychology*, 7, nov 2016. doi:10.3389/fpsyg.2016.01820.
- [5] Horace B. Barlow. *Representations of vision: trends and tacit assumptions in vision research*, chapter Vision tells you more than “What is Where”, pages 319–329. Cambridge University Press, Cambridge, 1991. ISBN 0-521-41228-5.
- [6] Nikolai Aleksandrovich Bernstein. *The co-ordination and regulation of movements*. Pergamon Press, Oxford, 1. English ed. edition, 1967.
- [7] Francis Crick and Chisato Asanuma. *Certain Aspects of the Anatomy and Physiology of the Cerebral Cortex*, volume 2, chapter 20, pages 333–371. The MIT Press, 1987. doi:10.7551/mitpress/5237.003.0011.
- [8] Sanjoy Dasgupta and Anupam Gupta. An elementary proof of a theorem of Johnson and Lindenstrauss. *Random Structures and Algorithms*, 22(1):60–65, nov 2002. doi:10.1002/rsa.10073.

- [9] Paul Dean, John Porrill, and James V. Stone. Decorrelation control by the cerebellum achieves oculomotor plant compensation in simulated vestibulo-ocular reflex. *Proceedings of the Royal Society of London. Series B: Biological Sciences*, 269 (1503):1895–1904, sep 2002. doi:10.1098/rspb.2002.2103.
- [10] Russell L. DeValois and Karen K. DeValois. *Spatial Vision*. Oxford University Press, jun 1991. ISBN 9780195066579. doi:10.1093/acprof:oso/9780195066579.001.0001.
- [11] David L. Donoho. De-Noising by Soft-Thresholding. *IEEE Transactions on Information Theory*, 41(3):613–627, May 1995. doi:10.1109/18.382009.
- [12] Miloš Doroslovački and Howard Fan. Wavelet-based linear system modeling and adaptive filtering. *IEEE Trans Signal Proc*, 44(5):1156–1167, May 1996.
- [13] Alexander S. Ecker, Philipp Berens, Georgios A. Keliris, Matthias Bethge, Nikos K. Logothetis, and Andreas S. Tolias. Decorrelated neuronal firing in cortical microcircuits. *Science*, 327(5965):584–587, jan 2010. doi:10.1126/science.1179867.
- [14] Jos J. Eggermont. *The Correlative Brain*. Springer Berlin Heidelberg, 1990. doi:10.1007/978-3-642-51033-5.
- [15] Peter Földiák. Forming sparse representations by local anti-Hebbian learning. *Biological Cybernetics*, 64(2):165–170, dec 1990. doi:10.1007/bf02331346.
- [16] Karl Friston, James Kilner, and Lee Harrison. A free energy principle for the brain. *J Physiol Paris*, 100:70–87, 2006. doi:10.1016/j.jphysparis.2006.10.001.
- [17] Masahiko Fujita. Adaptive filter model of the cerebellum. *Biol Cybern*, 45(3):195–206, 1982. ISSN 0340-1200. doi:10.1007/BF00336192.
- [18] Surya Ganguli and Haim Sompolinsky. Compressed sensing, sparsity, and dimensionality in neuronal information processing and data analysis. *Annu Rev Neurosci*, 35:485–508, March 2012. doi:10.1146/annurev-neuro-062111-150410.
- [19] Elad Ganmor, Ronen Segev, and Elad Schneidman. Sparse low-order interaction network underlies a highly correlated and learnable neural population code. *PNAS*, 108(23):9679–9684, June 2011. doi:10.1073/pnas.1019641108.
- [20] Peter Gärdenfors. *Conceptual spaces: the geometry of thought*. MIT Press, Cambridge, Mass., 2000. ISBN 0262071991.
- [21] Edward George Gray. Axo-somatic and axo-dendritic synapses of the cerebral cortex: An electron microscope study. *J Anat*, 93:420–433, 1959. URL <http://www.ncbi.nlm.nih.gov/pmc/articles/PMC1244535>.
- [22] Rick Greer. *A Tutorial On Polyhedral Convex Cones*, volume 96 of *North-Holland Mathematics Studies*, chapter 2, pages 15–81. North-Holland, 1984. doi:10.1016/S0304-0208(08)72857-3.
- [23] Paul R. Halmos. What Does the Spectral Theorem Say? *The American Mathematical Monthly*, 70(3):241, mar 1963. doi:10.2307/2313117.

- [24] Kristen M Harris and Richard J Weinberg. Ultrastructure of synapses in the mammalian brain. *Cold Spring Harb. Perspect. Biol.*, 4(a005587):1–30, feb 2012. doi:10.1101/cshperspect.a005587.
- [25] Simon S. Haykin. *Adaptive filter theory*. Prentice Hall, Upper Saddle River, N.J., 4. ed. edition, 2002. ISBN 0130901261.
- [26] John M Ingram and M.M Marsh. Projections onto convex cones in Hilbert space. *Journal of Approximation Theory*, 64(3):343–350, mar 1991. doi:10.1016/0021-9045(91)90067-k.
- [27] William B. Johnson and Joram Lindenstrauss. *Extensions of Lipschitz mappings into a Hilbert space*, volume 26, pages 189–206. American Mathematical Society, 1984. doi:10.1090/conm/026.
- [28] Thomas Kailath. An innovations approach to least-squares estimation—part i: Linear filtering in additive white noise. *IEEE Transactions on Automatic Control*, 13(6):646–655, dec 1968. doi:10.1109/tac.1968.1099025.
- [29] Mitsuo Kawato. Internal models for motor control and trajectory planning. *Curr Opin Neurobiol*, 9(6):718–727, Dec 1999. doi:10.1016/S0959-4388(99)00028-8.
- [30] Denis Kleyko, Dmitri A. Rachkovskij, Evgeny Osipov, and Abbas Rahimi. A survey on hyperdimensional computing aka vector symbolic architectures, part I: Models and data transformations. *ACM Computing Surveys*, 55(6):1–40, dec 2022. doi:10.1145/3538531.
- [31] Denis Kleyko, Dmitri Rachkovskij, Evgeny Osipov, and Abbas Rahimi. A survey on hyperdimensional computing aka vector symbolic architectures, part II: Applications, cognitive models, and challenges. *ACM Computing Surveys*, 55(9):1–52, jan 2023. doi:10.1145/3558000.
- [32] Wolfgang Köhler and Mary Henle. *The selected papers of Wolfgang Köhler*. Liveright, New York, 1971. ISBN 0-87140-505-9.
- [33] Adam Kohn, Ruben Coen-Cagli, Ingmar Kanitscheider, and Alexandre Pouget. Correlations and neuronal population information. *Annual Review of Neuroscience*, 39(1):237–256, jul 2016. doi:10.1146/annurev-neuro-070815-013851.
- [34] Teuvo Kohonen. *Associative Memory: A System-Theoretical Approach*. Springer, 1977. doi:10.1007/978-3-642-96384-1.
- [35] Teuvo Kohonen, Erkki Oja, and Pekka Lehtiö. *Storage and Processing of Information in Distributed Associative Memory Systems*, chapter 4, pages 125–167. Lawrence Erlbaum Associates, Hillsdale, NJ, 2nd edition, 1981.
- [36] Arvind Kumar, Stefan Rotter, and Ad Aertsen. Spiking activity propagation in neuronal networks: Reconciling different perspectives on neural coding. *Nature Rev Neurosci*, 11:615–624, Sept 2010. doi:10.1038/nrn2886.
- [37] Karl S. Lashley. *Brain Mechanisms and Intelligence*. University of Chicago Press, 1929.
- [38] Mark L. Latash. *Synergy*. Oxford University Press, mar 2008. doi:10.1093/acprof:oso/9780195333169.001.0001.

- [39] David G. Luenberger. *Optimization by vector space methods*. Wiley, New York, 1969. ISBN 047155359X.
- [40] Christian K. Machens, Ranulfo Romo, and Carlos D. Brody. Functional, but not anatomical, separation of “what” and “when” in prefrontal cortex. *The Journal of Neuroscience*, 30(1):350–360, jan 2010. doi:10.1523/jneurosci.3276-09.2010.
- [41] Bruce J. MacLennan. *Field Computation in the Brain*, chapter 7, pages 199–232. Psychology Press, apr 1993. doi:10.4324/9781315806570.
- [42] Bruce J. MacLennan. *Continuous Computation and the Emergence of the Discrete*, chapter 5, pages 121–152. Routledge, oct 1995. doi:10.4324/9781315789347-11.
- [43] Stéphane G. Mallat and Gabriel Peyré. *A wavelet tour of signal processing: the sparse way*. Elsevier/Academic Press, Burlington, Mass., 3rd edition, 2009. ISBN 9780123743701.
- [44] Chris J. McBain. Cortical inhibitory neuron basket cells: from circuit function to disruption. *The Journal of Physiology*, 590(4):667–667, feb 2012. doi:10.1113/jphysiol.2012.227967.
- [45] Hannes Mogensen, Johanna Norrlid, Jonas M. D. Enander, Anders Wahlbom, and Henrik Jörntell. Absence of repetitive correlation patterns between pairs of adjacent neocortical neurons *in vivo*. *Frontiers in Neural Circuits*, 13, jul 2019. doi:10.3389/fncir.2019.00048.
- [46] Martin N. P. Nilsson. Mechanistic explanation of neuronal plasticity using equivalent circuits. *bioRxiv*, May 2023. doi:10.1101/2023.05.21.541639.
- [47] Martin N. P. Nilsson and Henrik Jörntell. Channel current fluctuations conclusively explain neuronal encoding of internal potential into spike trains. *Phys. Rev. E*, 103:022407, Feb 2021. doi:10.1103/PhysRevE.103.022407.
- [48] Ann E. Nordmeyer and Michael C. Frank. Pragmatic felicity facilitates the production and comprehension of negation. *Collabra: Psychology*, 9(1), 2023. doi:10.1525/collabra.67931.
- [49] Richard J O’Brien, Sunjeev Kamboj, Michael D Ehlers, Kenneth R Rosen, Gerald D Fischbach, and Richard L Haganir. Activity-dependent modulation of synaptic AMPA receptor accumulation. *Neuron*, 21(5):1067–1078, nov 1998. doi:10.1016/s0896-6273(00)80624-8.
- [50] Erkki Oja. *Subspace methods of pattern recognition*. Research Studies Press, Letchworth, Herts., 1983. ISBN 0863800106.
- [51] Bruno A. Olshausen and David J. Field. Sparse coding with an overcomplete basis set: A strategy employed by V1? *Vision Research*, 37(23):3311–3325, dec 1997. doi:10.1016/s0042-6989(97)00169-7.
- [52] Bruno A. Olshausen and David J. Field. Sparse coding of sensory inputs. *Current Opinion in Neurobiology*, 14(4):481–487, aug 2004. doi:10.1016/j.conb.2004.07.007.

- [53] Günther Palm. Neural associative memories and sparse coding. *Neural Networks*, 37:165–171, jan 2013. doi:10.1016/j.neunet.2012.08.013.
- [54] Stefano Panzeri, Monica Moroni, Houman Safaai, and Christopher D. Harvey. The structures and functions of correlations in neural population codes. *Nature Reviews Neuroscience*, 23(9):551–567, jun 2022. doi:10.1038/s41583-022-00606-4.
- [55] Andras J. Pellionisz and Rodolfo Llinás. Tensor network theory of the metaorganization of functional geometries in the central nervous system. *Neuroscience*, 16(2):245–273, 1985. doi:10.1016/0306-4522(85)90001-6.
- [56] Donald H Perkel and Theodore Holmes Bullock. Neural coding. *Neurosciences Research Program Bulletin*, 6(3):219–349, December 1968.
- [57] Daniel A. Pollen, Jame R. Lee, and Joseph H. Taylor. How does the striate cortex begin the reconstruction of the visual world? *Science*, 173(3991):74–77, jul 1971. doi:10.1126/science.173.3991.74.
- [58] Roberto Quiñero, Gabriel Kreiman, Christof Koch, and Itzhak Fried. Sparse but not ‘grandmother-cell’ coding in the medial temporal lobe. *Trends in Cognitive Sciences*, 12(3):87–91, mar 2008. doi:10.1016/j.tics.2007.12.003.
- [59] Yoshio Sakurai. Population coding by cell assemblies—what it really is in the brain. *Neuroscience Research*, 26(1):1–16, sep 1996. doi:10.1016/0168-0102(96)01075-9.
- [60] Terence D Sanger. Neural population codes. *Current Opinion in Neurobiology*, 13(2):238–249, apr 2003. doi:10.1016/s0959-4388(03)00034-5.
- [61] Marco Santello, Gabriel Baud-Bovy, and Henrik Jörntell. Neural bases of hand synergies. *Front Comput Neurosci*, 7(23):1–15, 2013. ISSN 1662-5188. doi:10.3389/fncom.2013.00023.
- [62] Clifford B. Saper. Diffuse cortical projection systems: Anatomical organization and role in cortical function. *Comprehensive Physiology*, pages 169–210, dec 2011. doi:10.1002/cphy.cp010506.
- [63] Ali H. Sayed. *Fundamentals of adaptive filtering*. Wiley, Hoboken, N.J., 2003. ISBN 0471461261.
- [64] Wolfram Schultz and Anthony Dickinson. Neuronal coding of prediction errors. *Annual Review of Neuroscience*, 23(1):473–500, 2000. doi:10.1146/annurev.neuro.23.1.473. PMID: 10845072.
- [65] Vladimir M. Sloutsky and Yevgeniya Goldvarg. Mental representation of logical connectives. *The Quarterly Journal of Experimental Psychology Section A*, 57(4):636–665, may 2004. doi:10.1080/02724980343000413.
- [66] Terrence C. Stewart, Xuan Choo, and Chris Eliasmith. Symbolic reasoning in spiking neurons: A model of the cortex/basal ganglia/thalamus loop. In *Proceedings of the Annual Meeting of the Cognitive Science Society (CogSci’10)*, volume 32, pages 1100–1105, 2010. URL <https://escholarship.org/uc/item/81k1r713>.

- [67] Stephen F. Traynelis, Lonnie P. Wollmuth, Chris J. McBain, Frank S. Menniti, Katie M. Vance, Kevin K. Ogden, Kasper B. Hansen, Hongjie Yuan, Scott J. Myers, and Ray Dingledine. Glutamate receptor ion channels: Structure, regulation, and function. *Pharmacological Reviews*, 62(3):405–496, aug 2010. ISSN 0031-6997. doi:10.1124/pr.109.002451.
- [68] Koji Tsuda. The subspace method in Hilbert space. *Systems and Computers in Japan*, 32(6):55–61, 2001. doi:10.1002/scj.1034.
- [69] Vonne van Polanen. *Findings in Haptic (Re)search*. PhD thesis, VU University Amsterdam, 2014. ISBN: 978-94-6259-188-2.
- [70] Cornelis J. van Rijsbergen. *The Geometry of Information Retrieval*. Cambridge University Press, 2004. doi:10.1017/CBO9780511543333. URL <https://doi.org/10.1017/CBO9780511543333>.
- [71] John von Neumann. Probabilistic logics and the synthesis of reliable organisms from unreliable components. In *Automata Studies. (AM-34)*, pages 43–98. Princeton University Press, dec 1956. doi:10.1515/9781400882618-003.
- [72] John von Neumann. *The Computer and the Brain*. Yale University Press, dec 1958. ISBN 978-0300181111. doi:10.12987/9780300188080.
- [73] Anders Wahlbom, Jonas M. D. Enander, and Henrik Jörntell. Widespread decoding of tactile input patterns among thalamic neurons. *Frontiers in Systems Neuroscience*, 15, feb 2021. doi:10.3389/fnsys.2021.640085.
- [74] Satoshi Watanabe. *Knowing and Guessing: A Quantitative Study of Inference and Information*. John Wiley, New York, 1969. ISBN 0-471-92130-0.
- [75] Bernard Widrow and Marcian E. Hoff. Adaptive switching circuits. In *IRE WESCON Convention Record*, pages 96–104, Los Angeles, CA, August 1960. Institute of Radio Engineers, Institute of Radio Engineers. doi:10.21236/ad0241531. Part 4.
- [76] Bernard Widrow and Samuel D. Stearns. *Adaptive signal processing*. Prentice-Hall signal processing series. Prentice-Hall, Englewood Cliffs, N.J., 1985. ISBN 0-13-004029-0.
- [77] Herman O.A. Wold. *A Study in the Analysis of Stationary Time Series*. PhD thesis, Uppsala University, 1938.
- [78] Daniel M Wolpert, R Chris Miall, and Mitsuo Kawato. Internal models in the cerebellum. *Trends in Cognitive Sciences*, 2:338–347, 1998. doi:10.1016/S1364-6613(98)01221-2.
- [79] Byron M. Yu, John P. Cunningham, Gopal Santhanam, Stephen I. Ryu, Krishna V. Shenoy, and Maneesh Sahani. Gaussian-process factor analysis for low-dimensional single-trial analysis of neural population activity. *Journal of Neurophysiology*, 102(1):614–635, jul 2009. doi:10.1152/jn.90941.2008.
- [80] Wayne Xin Zhao, Kun Zhou, Junyi Li, Tianyi Tang, Xiaolei Wang, Yupeng Hou, Yingqian Min, Beichen Zhang, Junjie Zhang, Zican Dong, Yifan Du, Chen Yang, Yushuo Chen, Zhipeng Chen, Jinhao Jiang, Ruiyang Ren, Yifan Li, Xinyu Tang, Zikang Liu, Peiyu Liu, Jian-Yun Nie, and Ji-Rong Wen. A survey of large language models. *arXiv*, June 2023. doi:10.48550/arXiv.2303.18223.

- [81] Ehud Zohary, Michael N. Shadlen, and William T. Newsome. Correlated neuronal discharge rate and its implications for psychophysical performance. *Nature*, 370 (6485):140–143, jul 1994. doi:10.1038/370140a0.